Progress In Electromagnetics Research Letters, Vol. 91, 129–135, 2020

Filterless 16-Tupled Optical Millimeter-Wave Generation Using Cascaded Parallel Mach-Zehnder Modulators with Extinction Ratio Tolerance

Aasif B. Dar[1, *], Faroze Ahmad[1], and Rakesh K. Jha[2]

Abstract—A 16-tupling frequency system for millimeter-wave generation using cascaded arrangement of parallel Mach-Zehnder modulators is presented in this paper. Parallel non-ideal Mach-Zehnder modulators are used to realize a Mach-Zehnder modulator (MZM) with an ideal splitting ratio of 0.5. Hence, parallel MZMs work as a modulator with ultra-high extinction ratio. A 5 GHz radio frequency signal is 16-tupled to 80 GHz with optical sideband suppression ratio of 64 dB and radio frequency spurious sideband suppression ratio of 31 dB. The system has radio frequency spurious sideband suppression ratio $\geq$ 10 dB for modulation range of 2.79 to 2.86. Further, optical sideband suppression and radio frequency spurious sideband suppression ratios are independent of extinction ratio of MZMs.

1. INTRODUCTION

From the past decade, there has been accelerated penetration of wireless devices in the forms of smartphones, tablets, and laptops. Further, a large number of innovative applications run on these devices and require wireless data connection. To cater the emerging wireless bandwidth demands, it has been emphasized to transfer from existing microwave bands to millimeter-wave bands for next generation telecommunication [1]. However, generation and distribution of such high frequency signals using conventional techniques are cumbersome. Radio-over-fiber (RoF) technology provides an amalgam of high-bandwidth optical communication and adaptability with wireless communication [2]. Generation of high-quality mm-wave frequency signal and optimal design of transmission system of such signal along with data has been of great interest to researchers.

Various optical millimeter-wave (mm-wave) generation techniques have been proposed such as — Stimulated Brillouin scattering (SBS) [3], Four-Wave Mixing (FWM) [4, 5], Optical heterodyne [6–8], direct [9] and external modulation. Using SBS approach, the generation of frequency is limited to multiples of Brillouin frequency [10]. Stimulated Brillouin scattering is also known for the cause of performance degradation due to back-scattering of signal power. The frequency generation using FWM in nonlinear systems such as semiconductor optical amplifier (SOA) or highly non-linear fiber (HNLF) lacks operation stability. Optical heterodyne employing beating of two independent laser outputs using photo-detector provide simple system configuration. However, it results in poor phase noise characteristics due to mismatch of phases in two independent lasers. Direct modulation can be used for only low-frequency generation due to chirp and nonlinear effects [11]. Among the mentioned techniques, mm-wave generation by external modulation using MZMs offers higher reliability, frequency multiplication factor (FMF), and operation tunability.

Received 10 March 2020, Accepted 20 May 2020, Scheduled 3 June 2020
* Corresponding author: Aasif Bashir Dar (daraasifshzd@gmail.com).
[1] Department of Electronics and Communication Engineering, IUST Awantipora, J&K, India. [2] Department of Electronics and Communication Engineering, SMVDU Katra, J&K, India.

FMFs of four [11, 12], six [13], and eight [14] have been proposed, but lower FMF requires a high frequency RF oscillator to generate higher frequency mm-wave signal. Systems with higher FMFs of 12, 16, 18 have been proposed at modulation index (MI) greater than five, which increases system sensitivity [15–17]. Filterless 16-tupling mm-wave generation has been proposed using cascaded MZMs with assumption of the extinction ratio of 100 dB, which is not realizable [18]. Several mm-wave frequency generation schemes employing filters have also been proposed. However, the use of optical filters increases the complexity of a system.

The remainder of the paper is arranged as follows. Section 2 presents the operation principle for 16 frequency tupling using parallel MZMs. Section 3 provides results along with discussion. Conclusion is provided in Section 4.

2. PRINCIPLE

In this section, realization of an ideal splitting ratio MZM using parallel non-ideal MZMs is discussed first. Later, application of this ideal splitting ratio MZM in generation of 16-tupled mm-wave is presented.

2.1. Realization of Ideal Splitting Ratio MZM

The schematic diagram for realization of ideal splitting ratio MZM using dual-parallel MZMs shown in Figure 1(b).

The output of MZM can be written as [19];

$$E_{oMZM}(t) = \alpha E_i(t)\left[\gamma e^{j\pi\left(\frac{v_2(t)}{v_\pi}+\frac{v_{bias2}}{v_\pi}\right)} + (1-\gamma)\, e^{j\pi\left(\frac{v_1(t)}{v_\pi}+\frac{v_{bias1}}{v_\pi}\right)}\right] \tag{1}$$

where α is the attenuation factor due to insertion loss; $\gamma = \frac{\left(1-\frac{1}{\sqrt{\epsilon_r}}\right)}{2}$ (where $\epsilon_r = 10^{(Extinction\,Ratio)/10}$) is the power splitting ratio of two arms; and V_π is the half wave voltage of MZM. For an ideal MZM $\gamma = 0.5$, which corresponds to infinite extinction ratio. Consider that the light signal $E_0 e^{j\omega_c t}$ emitted from the laser diode (LD) is fed to MZM with splitting ratio of 'γ' as shown in Figure 1(a). Let $(1-\gamma) = \beta$, and for MZM operating at maximum transmission point $v_{bias1} = v_{bias2} = 0$. Eq. (1) can be reduced as

$$E_{oMZM}(t) = \alpha E_i(t)\left[\gamma e^{jm\sin(\omega_m t+\pi)} + \beta e^{jm\sin(\omega_m t)}\right] \tag{2}$$

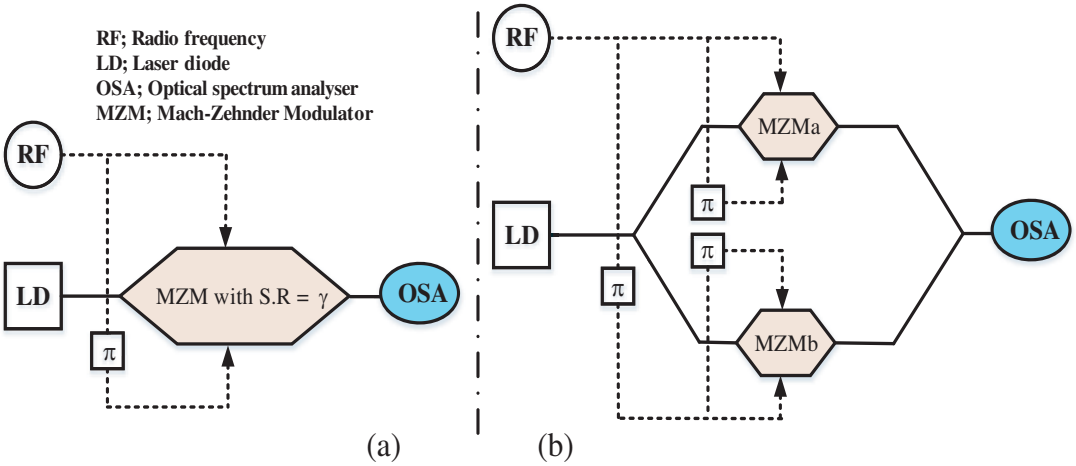

Figure 1. (a) Practical MZM with arbitrary any splitting ratio (γ). (b) Schematic diagram for realization of MZM with splitting ratio (γ) ≈ 0.5.

where $m = \frac{\pi v_m}{v_\pi}$ is the Modulation Index. Jacobi-Anger expansions are written as

$$e^{jm\sin\Theta} = \sum_{n=-\infty}^{\infty} J_n(m)\, e^{jn\Theta}; \quad e^{jm\cos\Theta} = \sum_{n=-\infty}^{\infty} j^n J_n(m)\, e^{jn\Theta} \tag{3}$$

Therefore, using Jacobi-Anger expansions Eq. (2) can be simplified as

$$E_{oMZM}(t) = \alpha E_i(t)\left[\gamma \sum_{n=-\infty}^{\infty} J_n(m) e^{jn(\omega_m t+\pi)} + \beta \sum_{n=-\infty}^{\infty} J_n(m) e^{jn(\omega_m t)}\right] \tag{4}$$

$$E_{oMZM}(t) = \alpha E_0 e^{j\omega_c t} \sum_{n=-\infty}^{\infty} J_n(m)\, e^{jn\omega_m t}[(-1)^n\gamma + \beta] \tag{5}$$

Eq. (5) suggests the presence of all harmonics. However, the power of odd harmonics is less because of (β-γ) factor. Further, as the order of Bessel function increases the strength of the term decreases, because $J_n(m)$ is the decreasing function with respect to n and m. However, if the MZM is ideal, i.e., $\gamma = \beta = 0.5$, Eq. (5) can be simplified as;

$$E_{oMZM}(t) \propto E_0 e^{j\omega_c t} \sum_{n=-\infty}^{\infty} J_{2n}(m)\, e^{j2n\omega_m t} \tag{6}$$

Eq. (6) suggests the presence of even harmonics, which is an ideal case for MZM at maximum transmission point (MTP).

Similarly, the output of system shown in Figure 1(b) can be given as

$$\begin{aligned} E_o(t) \;\propto\; & E_i(t)\left[\gamma e^{j\pi\left(\frac{v_{2a}(t)}{v_\pi}+\frac{v_{bias2}}{v_\pi}\right)} + (1-\gamma)\, e^{j\pi\left(\frac{v_{1a}(t)}{v_\pi}+\frac{v_{bias1}}{v_\pi}\right)}\right] \\ & + E_i(t)\left[\gamma e^{j\pi\left(\frac{v_{2b}(t)}{v_\pi}+\frac{v_{bias2}}{v_\pi}\right)} + (1-\gamma)\, e^{j\pi\left(\frac{v_{1b}(t)}{v_\pi}+\frac{v_{bias1}}{v_\pi}\right)}\right] \end{aligned} \tag{7}$$

For MZM-a; $v_{1a}(t) = v_m\sin(\omega_m t)$ and $v_{2a}(t) = v_m\sin(\omega_m t+\pi)$ and for MZM-b; $v_{1b}(t) = v_m\sin(\omega_m t+\pi)$ and $v_{2b}(t) = v_m\sin(\omega_m t)$. $V_{bias} = 0\,\mathrm{V}$ for all MZMs. Hence Eq. (3) can be further solved to

$$\begin{aligned} E_o(t) \;\propto\; & E_i(t)\left\{\left[\gamma e^{jm\sin(\omega_m t+\pi)} + (1-\gamma)\, e^{jm\sin(\omega_m t)}\right] + \left[\gamma e^{jm\sin(\omega_m t)} + (1-\gamma)\, e^{jm\sin(\omega_m t+\pi)}\right]\right\} \\ \propto\; & E_0 e^{j\omega_c t}\left\{\left[\gamma \sum_{n=-\infty}^{\infty} J_n(m) e^{jn(\omega_m t+\pi)} + (1-\gamma) \sum_{n=-\infty}^{\infty} J_n(m) e^{jn(\omega_m t)}\right]\right. \\ & \left. + \left[\gamma \sum_{n=-\infty}^{\infty} J_n(m) e^{jn(\omega_m t)} + (1-\gamma) \sum_{n=-\infty}^{\infty} J_n(m) e^{jn(\omega_m t+\pi)}\right]\right\} \end{aligned} \tag{8}$$

Eq. (8) can be further simplified as

$$E_o(t) \propto E_0 e^{j\omega_c t} \sum_{n=-\infty}^{\infty} J_{2n}(m)\, e^{j2n(\omega_m t)} \tag{9}$$

Eq. (9) suggests the presence of only even order side bands, as that of an ideal MZM at MTP.

2.2. Frequency 16-Tupling

The schematic diagram for a 16-tupling system using the ideal MZM realized in Section 2.1 is shown in Figure 2.

The output after th efirst MZM is given by Eq. (9), which acts as an input to next MZM. The outputs of the 2nd and 3rd MZMs act as the inputs to the 3rd and 4th MZMs, respectively. Therefore,

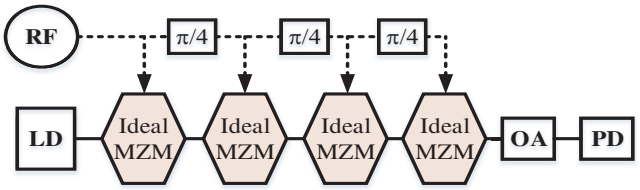

Figure 2. Schematic diagram 16-tupling mm-wave generation system. OA; optical amplifier, PD; photodiode.

output after the cascaded arrangement of modulators can be given as

$$E_o(t) \propto E_0 e^{j\omega_c t}\left\{\left[\sum_{n=-\infty}^{\infty} J_{2n}(m)\, e^{j2n(\omega_m t)}\right]\times\left[\sum_{n=-\infty}^{\infty} J_{2n}(m)\, e^{j2n(\omega_m t)} e^{jn\frac{\pi}{2}}\right]\right.$$
$$\left.\times\left[\sum_{n=-\infty}^{\infty} J_{2n}(m) e^{j2n(\omega_m t)} e^{jn\pi}\right]\times\left[\sum_{n=-\infty}^{\infty} J_{2n}(m) e^{j2n(\omega_m t)} e^{jn\frac{3\pi}{2}}\right]\right\} \quad (10)$$

Upon expansion of each summation term, Eq. (10) can be written as

$$\begin{aligned} E_o(t) \propto\ & E_0 e^{j\omega_c t}\{[J_0(m) + 2J_2(m)\cos(2\omega_m t) + 2J_4(m)\cos(4\omega_m t) + 2J_6(m)\cos(6\omega_m t) + \ldots] \\ & \times [J_0(m) - 2J_2(m)\sin(2\omega_m t) - 2J_4(m)\cos(4\omega_m t) + 2J_6(m)\sin(6\omega_m t) - \ldots] \\ & \times [J_0(m) - 2J_2(m)\cos(2\omega_m t) + 2J_4(m)\cos(4\omega_m t) - 2J_6(m)\cos(6\omega_m t) + \ldots] \\ & \times [J_0(m) + 2J_2(m)\sin(2\omega_m t) - 2J_4(m)\cos(4\omega_m t) - 2J_6(m)\sin(6\omega_m t) + \ldots]\} \end{aligned} \quad (11)$$

Neglecting higher order terms in each of the expansions as $J_n(m)$ is decreasing function with respect to 'n' and 'm', Eq. (11) can be reduced as

$$E_o(t) \propto E_0 e^{j\omega_c t}\left\{\left[A^2 - \frac{B^2}{2} + \frac{D^2}{2} - \frac{F^2}{2}\right] + \left[2AD - \frac{B^2}{2} - BF\right]\cos(8\omega_m t)\right.$$
$$\left. + \left[\frac{D^2}{2} - BF\right]\cos(16\omega_m t) - \frac{F^2}{2}\cos(24\omega_m t)\right\} \quad (12)$$

where $A = \left[J_0^2(m) - 2J_2^2(m) + 2J_4^2(m) - 2J_6^2(m)\right]$, $B = \left[2J_2^2(m) - 4J_0(m)J_4(m) + 4J_2(m)J_6(m)\right]$, $D = \left[2J_4^2(m) - 4J_2(m)J_6(m)\right]$ and $F = 2J_6^2(m)$. Eq. (12) reflects the presence of ω_c and $(\omega_c \pm 8n\omega_m)$ frequency components in the output of cascaded arrangements of MZMs. Figure 3(a) shows the plot of coefficients of ω_c and $(\omega_c + 8n\omega_m)$ frequency components in Eq. (12) with respect to modulation index 'm'. The values of coefficients for the 16th and 24th harmonic frequencies are zero for the modulation index range of 0 to 5. So only ω_c and $(\omega_c + 8\omega_m)$ frequency components will be under consideration for the further discussion.

3. RESULTS AND DISCUSSION

Figure 3(b) shows the variation of calculated band power ratio (P_0/P_8) with modulation index, using Eq. (12). In the figure, around modulation index of 1.6, 1.9, and 2.8, $(\frac{P_0}{P_8})$ is minimum, reflecting that the cascaded arrangement of parallel MZMs works as a frequency 16-tupling system. However, around modulation index of 1.6 and 1.9, P_8 is low, and $(\frac{P_8}{P_0})$ is more sensitive to biasing variations as suggested by Figure 3. Therefore, biasing is adjusted such that modulation index is around 2.8. Analytical calculations show that at $m = 2.828$, $(\frac{P_8}{P_0}) \approx 63$ dB.

$$\frac{P_8}{P_0}_{at\ m=2.828} = 10\log_{10}\left\{\frac{\left[A^2 - \frac{B^2}{2} + \frac{D^2}{2} - \frac{F^2}{2}\right]^2}{\left[AD - \frac{B^2}{4} - \frac{BF}{2}\right]^2}\right\} = 62.4041\,\text{dB} \quad (13)$$

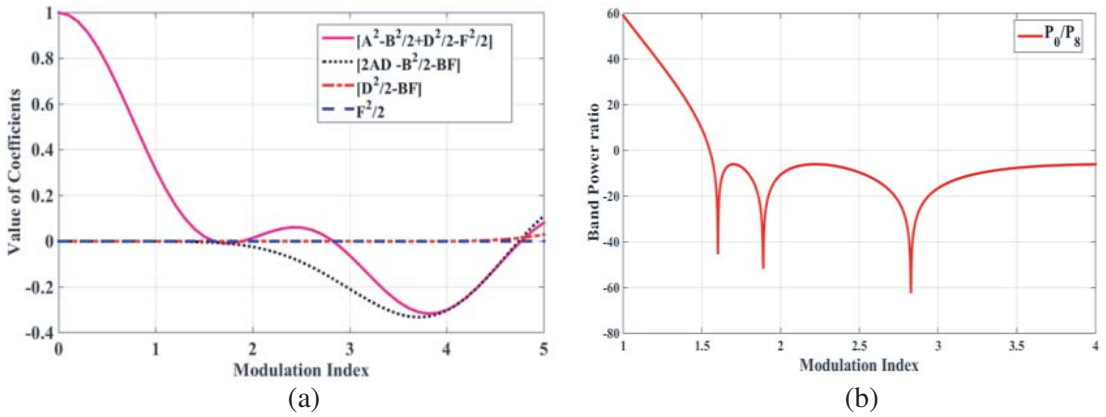

Figure 3. (a) Variation of frequency coefficients with modulation Index. (b) Variation of band power ratio with modulation Index.

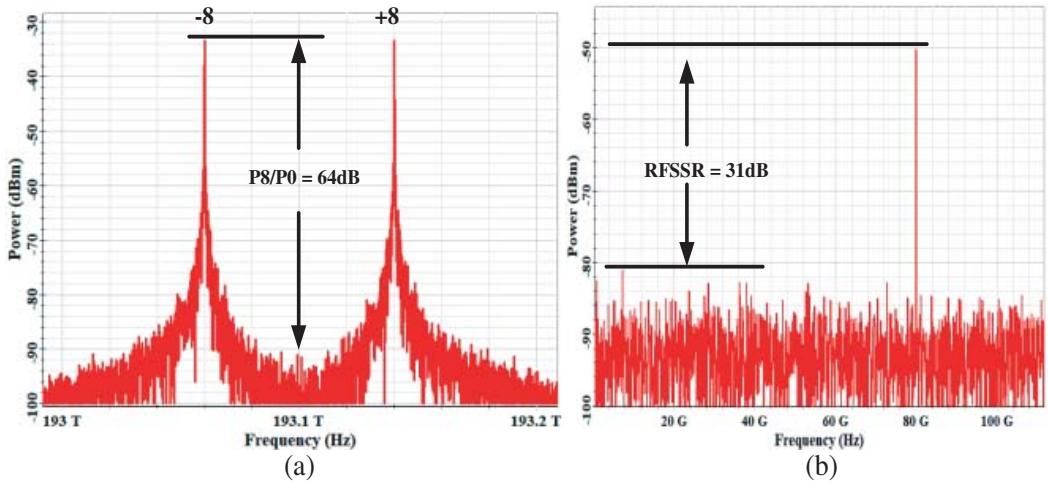

Figure 4. (a) Optical spectrum and (b) RF spectrum, at $m = 2.8274$.

However, system shows $(\frac{P_8}{P_0}) \approx 64\,\text{dB}$ at the $m = 2.8274$. This small deviation from the mathematical calculation can be explained as Eq. (12) is resultant from multiplication of truncated expansions, hence is an approximate relation. Figure 4 shows the optical spectrum and radio frequency spectrum after the detection of system at the modulation index of 2.8274.

Figure 5(a) shows the variations of OSSR and RFSSR with modulation index. The system provides OSSR $\geq 10\,\text{dB}$ in the modulation index range of 2.75–2.90. The system provides the peak OSSR and RFSSR of 64 dB and 31 dB, respectively, at the modulation index of 2.8274. Figure 5(b) shows the variation of OSSR and RFSSR with extinction ratio of parallel MZMs. As long as extinction ratio of parallel MZMs is same, the output of system is not affected.

In the proposed system setup there are three '$\pi/4$' phase shifter and four ideal MZMs. Further, an ideal MZM was realized using parallel MZMs and three 'π' phase shifters. To evaluate the effect of phase offset on system performance, variation of OSSR with phase offset in phase shifters is analyzed. Figure 6 shows the variation of OSSR with phase offset in 'π' phase shifters and '$\pi/4$' phase shifter. It can be noted that for $\pm 10^\circ$ phase offset in 'π' phase shifters, OSSR is well above 20 dB reflecting that the system is tolerant to phase variation as far as 'π' phase shifters are considered. The system is relatively sensitive to phase offset in '$\pi/4$' phase shifter. However, the performance is acceptable for $\pm 5^\circ$ phase offset.

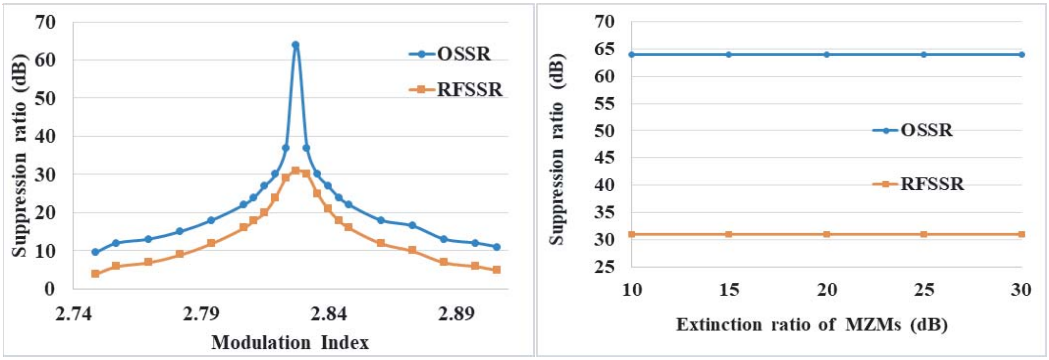

Figure 5. (a) Variation of OSSR and RFSSR with Modulation index 'm'. (b) Variation of OSSR and RFSSR with extinction ratio of parallel MZMs.

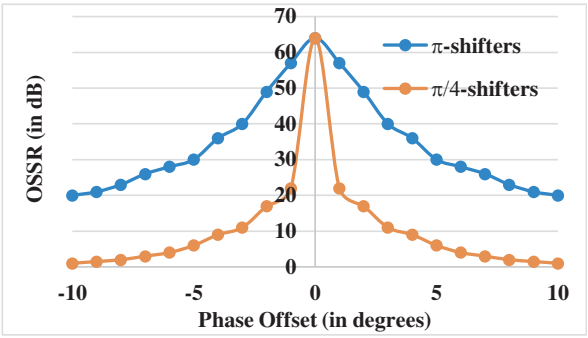

Figure 6. Variation of OSSR with phase offset in phase shifters.

4. CONCLUSION

A novel 16-tupled mm-wave generation system operating at lower modulation index for MZMs is presented in this paper. MZM with splitting ratio of 0.5 is realized with two parallel non-ideal MZMs. The demonstration of generation of 80 GHz signal from 5 GHz RF source is done. However, the system architecture is general, and hence the generation of any required mm-wave can be achieved by controlling the frequency RF source. For example, 60 GHz can be generated using 3.75 GHz RF source. Using proper biasing adjustments, a high-quality mm-wave can be generated. The OSSR and RFSSR are constant with variation of extinction ratio of MZMs.

ACKNOWLEDGMENT

The authors would like to acknowledge the communication lab SMVDU for providing lab support.

REFERENCES

1. Chen, S. and J. Zhao, "The requirements, challenges, and technologies for 5G of terrestrial mobile telecommunication," *IEEE Communications Magazine*, Vol. 52, No. 5, 36–43, May 2014.
2. Jia, Z., J. Yu, G. Ellinas, and G. Chang, "Key enabling technologies for optical-wireless networks: Optical millimeter-wave generation, wavelength reuse, and architecture," *Journal of Lightwave Technology*, Vol. 25, No. 11, 3452–3471, Nov. 2007.

3. Yan, J., A. Liang, F. Xin, and Q. Liu, "An optical microwave generator based on stimulated brillouin scattering with fine tunability," *Conference on Lasers and Electro-Optics*, OSA Technical Digest (online) (Optical Society of America, 2018), JW2A.181, 2018.
4. Zhang, C., L. Wang, and K. Qiu, "Proposal for all-optical generation of multiple-frequency millimeter-wave signals for RoF system with multiple base stations using FWM in SOA," *Opt. Express*, Vol. 19, 13957–13962, 2011.
5. Wang, T., M. Chen, H. Chen, and S. Xie, "Millimetre-wave signal generation using FWM effect in SOA," *Electronics Letters*, Vol. 43, No. 1, 36–38, Jan. 4, 2007.
6. Stohr, R. H., A. Malcoci, and D. Jager, "Optical heterodyne millimeter-wave generation using 1.55-/spl mu/m traveling-wave photodetectors," *IEEE Transactions on Microwave Theory and Techniques*, Vol. 49, No. 10, 1926–1933, Oct. 2001.
7. Browning, C., A. Delmade, Y. Lin, D. H. Geuzebroek, and L. P. Barry, "Optical heterodyne millimeter-wave analog radio-over-fiber with photonic integrated tunable lasers," *Optical Fiber Communication Conference (OFC) 2019*, OSA Technical Digest (Optical Society of America, 2019), W1I.4, 2019.
8. Li, X., J. Xiao, Y. Xu, and J. Yu, "QPSK vector signal generation based on photonic heterodyne beating and optical carrier suppression," *IEEE Photonics Journal*, Vol. 7, No. 5, 1–6, Oct. 2015.
9. Chen, L., Y. Pi, H. Wen, and S. Wen, "All-optical mm-wave generation by using direct-modulation DFB laser and external modulator," *Microw. Opt. Technol. Lett.*, Vol. 49, 1265–1267, 2007.
10. Zhu, Z., S. Zhao, W. Zheng, W. Wang, and B. Lin, "Filterless frequency 12-tupling optical millimeter-wave generation using two cascaded dual-parallel Mach-Zehnder modulators," *Appl. Opt.*, Vol. 54, 9432–9440, 2015.
11. He, Y., Y. Li, Y. Cai, X. Zhang, J. Liu, J. Xiao, S. Chen, and D. Fan, "A full-duplex 100-GHz radio-over-fiber communication system based on frequency quadrupling," *Optik*, Vol. 175, 148–153, 2018.
12. Yu, S., W. Gu, A. Yang, T. Jiang, and C. Wang, "A frequency quadrupling optical mm-Wave generation for hybrid fiber-wireless systems," *IEEE Journal on Selected Areas in Communications*, Vol. 31, No. 12, 797–803, Dec. 2013.
13. Mohamed, M., X. Zhang, B. Hraimel, and K. Wu, "Frequency sixupler for millimeter-wave over fiber systems," *Opt. Express*, Vol. 16, 10141–10151, 2008.
14. Ma, J., X. Xin, J. Yu, C. Yu, K. Wang, H. Huang, and L. Rao, "Optical millimeter wave generated by octupling the frequency of the local oscillator," *J. Opt. Netw.*, Vol. 7, 837–845, 2008.
15. Li, X., S. Zhao, Z. Zhu, B. Gong, X. Chu, Y. Li, J. Zhao, and Y. Liu, "An optical millimeter-wave generation scheme based on two parallel dual-parallel Mach-Zehnder modulators and polarization multiplexing," *Journal of Modern Optics*, Vol. 62, No. 18, 1502–1509, 2015.
16. Chen, Y., A. Wen, J. Guo, L. Shang, and Y. Wang, "A novel optical mm-wave generation scheme based on three parallel Mach-Zehnder modulators," *Opt. Commun.*, Vol. 284, No. 5, 1159–1169, 2011.
17. Zhu, Z., S. Zhao, Y. Li, X. Chu, X. Wang, and G. Zhao, "A radio-over-fiber system with Frequency 12-tupling optical millimeter-wave generation to overcome chromatic dispersion," *IEEE J. Quantum Electron.*, Vol. 49, No. 11, 919–922, 2013.
18. Baskaran, M. and R. Prabakaran, "Optical millimeter wave signal generation with frequency 16-tupling using cascaded MZMs and no optical filtering for radio over fiber system," *Journal of the European Optical Society-Rapid Publications*, Vol. 14, 13, 2018.
19. Dar, A. B. and F. Ahmad, "A full-duplex 40 GHz radio-over-fiber transmission system based on frequency octupling," *Optical and Quantum Electronics*, Vol. 51, 324, 2019.